Article ID: 1000-7032(2025)12-2293-09

Design, Synthesis and Optoelectronic Properties of Bipolar Host Materials Based on 9-penylcarbazole and Benzimidazole

HUANG Hong[1*], XIONG Zhangqi[1], DENG Depeng[1], XIA Weimin[1], ZHANG Youming[1], HUA Tao[1], LI Nengquan[1], XIE Guohua[2*]

(1. *Institute of Technology for Future Industry, School of Science and Technology Instrument Application Engineering, Shenzhen University of Information Technology, Shenzhen* 518172, *China*;
2. *Institute of Flexible Electronics (IFE, Future Technologies), Institute of Future Display Technology, Tan Kah Kee Innovation Laboratory, Xiamen University, Xiamen* 361102, *China*)
* *Corresponding Authors, E-mail: huangxiaoli*1985@126.*com*; *ifeghxie@xmu.edu.cn*

Abstract: Theoretically, blue phosphorescent materials are capable of achieving 100% internal quantum efficiency. Nevertheless, the mutual constraints among efficiency, color purity, and stability remain one of the key bottlenecks in the industrialization of organic light-emitting diodes (OLEDs). In addition, the design and application of host materials also exert a significant impact on the overall performance of blue light-emitting devices. To address this issue, this study constructs a series of host materials with high triplet energy levels by designing different connection modes, based on 9-phenylcarbazole and benzimidazole units. Through a combination of theoretical and experimental approaches, the correlation between the chemical structure and performance has been unraveled. It is found that the designed and synthesized blue phosphorescent bipolar host materials based on different biphenyl linking sites, *i.e.*, 9-(3′-(1-phenyl-1H-benzo[d]imidazol-2-yl)-[1,1′-biphenyl]-3-yl)-9H-carbazole(**mCzmBI**), 9-(2′-(1-phenyl-1H-benzo[d]imidazol-2-yl)-[1,1′-biphenyl]-3-yl)-9H-carbazole(**mCzoBI**) and 9-(3′-(1-phenyl-1H-benzo[d]imidazol-2-yl)-[1,1′-biphenyl]-2-yl)-9H-carbazole (**oCzmBI**). The three compounds have a similar triplet energy level of 2.70 eV, accompanied with the glass transition temperatures of 92 ℃, 103 ℃, and 93 ℃ respectively. **mCzmBI**, **mCzoBI** and **oCzmBI** are regioisomers, but differ in the linking sites of carbazole and benzimidazole on the biphenyl linker. This difference in linking positions enables effective regulation of the host materials' properties. Constructed with the blue phosphorescent material bis(4,6-difluorophenylpyridinato-N,C2)picolinatoiridium(Ⅲ)(FIrpic) as the guest, the influence of the three hosts on device performance is clarified. Overall, the device using **mCzmBI**, a host linked by biphenyl at double meta-positions, achieved a maximum current efficiency of 24.9 $cd \cdot A^{-1}$ and a maximum external quantum efficiency exceeding 12.8%, it also demonstrates low efficiency roll-off under high-brightness conditions. This work offers an effective strategy to the development of high-efficiency blue phosphorescent hosts.

Key words: blue phosphorescent; organic electroluminescence; 9-phenylcarbazole; benzimidazole; host materials
CLC number: O482.31 **Document code**: A
DOI: 10.37188/CJL.20250223 **CSTR**: 32170.14.CJL.20250223

收稿日期: 2025-10-02; **修订日期**: 2025-10-13
基金项目: 深圳市科技计划项目(20231127123500001, 20231127120511001, JCYJ20240813143022029); 深圳信息职业技术大学项目(TD2024E002, SZIIT2025KJ045, SZIIT2024KJ021); 国家自然科学基金(52373195, 62175189, 22405177); 广东省基础研究与应用基础研究基金(20205A1515010054)
Supported by Shenzhen Science and Technology Program (20231127123500001, 20231127120511001, JCYJ20240813143022029); Shenzhen Universtiy of Information Technology (TD2024E002, SZIIT2025KJ045, SZIIT2024KJ021); National Natural Science Foundation of China (5237319, 22405177, 62175189); Guangdong Basic and Applied Basic Research Foundation (2025A1515010054)

含 9-苯基咔唑与苯并咪唑单元的双极主体材料设计、合成及其光电性能

黄 宏[1*]，熊章奇[1]，邓德朋[1]，夏位敏[1]，张友明[1]，华 涛[1]，李能泉[1]，谢国华[2*]

（1. 深圳信息职业技术大学 未来产业技术研究院，科技仪器应用工程学院，广东 深圳 518172；
2. 厦门大学柔性电子（未来技术）研究院，厦门市未来显示技术研究院，嘉庚创新实验室，福建 厦门 361102）

摘要：蓝色磷光材料理论上可实现 100% 的内量子效率，但其效率、色纯度、稳定性三者之间的相互制约关系仍是有机发光二极管（OLED）产业化进程中的关键瓶颈之一。此外，主体材料的设计和使用在很大程度上也影响了蓝光器件的整体性能。为此，本研究以 9-苯基咔唑与苯并咪唑单元为基础，通过设计不同连接方式构建高三线态能级主体材料，采用理论与实验相结合的方法，探究材料的分子结构、光物理性能及器件应用性能，揭示其结构与性能之间的关联。实验结果表明，所设计并制备的基于不同联二苯基连接位点的蓝色磷光双极主体材料（即 **mCzmBI**、**mCzoBI** 与 **oCzmBI**）均具有 2.70 eV 的三线态能级，三者的玻璃化转变温度分别为 92 ℃、103 ℃和 93 ℃。虽然 **mCzmBI**、**mCzoBI** 与 **oCzmBI** 互为同分异构体，但其咔唑基团与苯并咪唑基团在联苯基团上的连接位点不同，这种连接位点的差异可以很好地实现对主体材料性能的有效调控。以经典蓝光磷光材料 FIrpic 为客体，分别研究三种主体对器件性能的影响机制。其中，以联二苯基双间位连接的主体 **mCzmBI** 所构筑的器件最大电流效率达 24.9 $cd\cdot A^{-1}$，最大外量子效率超过 12.8%，并在高亮度环境下表现出较低的效率滚降。该研究为高效蓝光磷光主体的开发提供了一种有效的策略。

关 键 词：蓝色磷光；有机电致发光；9-苯基咔唑；苯并咪唑；主体材料

1 Introduction

Since the first demonstration of the advantages of phosphorescent organic light-emitting diodes (PhOLEDs) in 1998, the development of high-performance phosphorescent host materials has emerged as a core driving force in this research field[1]. Theoretically, phosphorescent materials can achieve 100% internal quantum efficiency. Meanwhile, driven by the widespread adoption of OLED smartphones and the urgent demand for longer battery life, the development of high-efficiency all-phosphorescent devices has become one of the key focuses in both academia and industry. The emissive layer structure of PhOLEDs generally contains triplet phosphorescent guest and host materials, and the physicochemical, electrical, and thermodynamic properties of both play a key role in the device performance[1]. Bipolar host materials constructed from electron-rich and electron-deficient units rank as the most optimal phosphorescent host materials for practical use[2-3]. Over the past decades, researchers have continuously optimized and refined the design of such materials, aiming to bring the performance of PhOLEDs to meet the requirements of practical application. To date, while phosphorescent host materials for red and green PhOLEDs have grown increasingly mature in design and development, the blue host-guest system still does not satisfy the rigorous industrial requirements for practical applications[3-10]. A major merit of donor/acceptor-type host materials resides in their capacity for bipolar charge transport, establishing them as a universal approach to host material design. Specifically, in 2020, the reported host material SPA-2,7-F$(POPh_2)_2$ achieved an ideal balance between hole mobility (8.2×10^{-6} $cm^2\cdot V^{-1}\cdot s^{-1}$) and electron mobility (2×10^{-4} $cm^2\cdot V^{-1}\cdot s^{-1}$). This balanced transport property stabilizes carrier injection in the emissive layer, thereby elevating the probability of radiative recombination[8,11]. Owing to this inherent characteristic, SPA-2,7-F$(POPh_2)_2$ has been successfully employed in single-layer

PhOLEDs, achieving a maximum external quantum efficiency of 18%. Notably, this device architecture obviates the requirement for extra functional transport layers, thereby facilitating streamlined device fabrication and lowering manufacturing costs.

At present, achieving high-efficiency and stable blue PhOLEDs remains a key bottleneck that the OLED industry must address urgently. Overall, blue OLEDs——regardless of their emission mechanism (fluorescence, phosphorescence, thermally activated delayed fluorescence, or superfluorescence)[12-15]——have consistently been a limiting factor in the advancement of this technology [3,16-22]. For organic molecules, high triplet energy and superior bipolar charge transport performance typically present an inherent incompatibility. The root cause lies in the introduction of electron-donating (D) and electron-withdrawing (A) groups, which tends to initiate intramolecular charge transfer; this process in turn reduces the band gap and leads to a decline in the triplet energy level. Thus, in the development of bipolar host materials with high triplet energy levels, developing an effective strategy to minimize electronic coupling between D and A moieties is of utmost urgency.

For the development of bipolar host materials with high triplet energy levels, researchers have developed various strategies, though these methods primarily center on suppressing electron transfer between D and A moieties to obtain the target performance. In this investigation, we designed three new bipolar host materials (**mCzmBI**, **mCzoBI**, and **oCzmBI**) by utilizing the unique advantage of highly twisted molecular conformations. One of the feature characteristics is the introduction of the suitable D and A units at the 2,2′- or 2,3′-position of the biphenyl linker since carbazole with hole transport ability and benzimidazole with electron transport ability[23-24], which provides an effective reference for exploring the effect of different effective conjugation degrees and triplet energy levels on the structure-property relationship of materials. Notably, **mCzmBI**, **mCzoBI**, and **oCzmBI** exhibited regioisomeric characteristics, with specific differences in the connection sites between benzimidazole and 9-phenylcarbazole. This structural feature is conducive to maintaining high triplet energy levels, thereby holding promise for fabricating PhOLEDs with enhanced efficiency. We conducted a comparative study on the thermodynamic, photophysical, and electrochemical properties of these three host materials in combination with their molecular structures, and fabricated blue phosphorescent devices using **mCzmBI**, **mCzoBI**, and **oCzmBI** as hosts, respectively. The device with **mCzmBI** exhibited best efficiency with lower efficiency roll-off. The maximum external quantum efficiencies of the three blue PhOLEDs reached 12.8%, 8.4%, and 11.0%, respectively.

2　Results and Discussion

2.1　Synthesis and Characterization

Fig. 1 shows the experimental synthesis routes and specific synthetic procedures that the synthesis of benzimidazole- and carbazole-based phosphorescent host compounds is straightforward. All compounds can be synthesized in only one to two reaction steps from the starting materials to the final products (refer to the synthesis and characterization section in the SI[25-28]). Notably, the last step is the classic Suzuki reaction, which affords high yields. Although the ortho-substitution increases the steric repulsion between groups, the yield still exceeds 50%. All host compounds were finally purified using a vacuum sublimator, and the structures of all bipolar phosphorescent host compounds were characterized by ^{1}H-NMR, ^{13}C-NMR, and mass spectrometry.

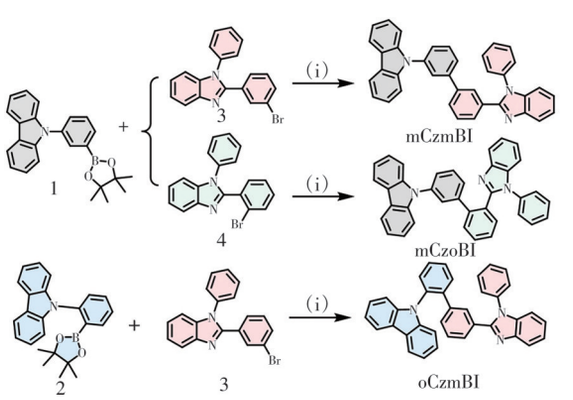

Fig.1　Synthetic routes of **mCzmBI**, **mCzoBI** and **oCzmBI**. (i) $Pd(PPh_3)_4$, K_2CO_3 (2.0 mol·L^{-1}), protected from light for 12 h, 100 ℃

Owing to the presence of benzimidazole groups, all benzimidazole-carbazole-based bipolar phosphorescent host compounds are highly soluble in common solvents, such as dichloromethane, toluene, and chloroform.

2.2 Photophysical Properties

Fig. 2 presents the UV-Vis absorption and fluorescence emission spectra of biphenyl-linked carbazole-based bipolar phosphorescent host compounds in dilute dichloromethane solutions. For absorption spectra of these host compounds, all exhibit an absorption in the wavelength range of 250–360 nm, with the maximum absorption consistently observed at 250 nm of the three compounds. This absorption can be attributed to the n-π^* transition of the biphenyl moiety. Additionally, a distinct absorption peak appeared at 290 nm, which arose from the n-π^* transition within the carbazole segment. Based on the analysis the absorption in the range of 300–360 nm, it is clear that, when the biphenyl groups are linked at the para position, the corresponding host compound showed relatively stronger absorption, compared with that with biphenyl linkages at the ortho or meta positions. This phenomenon is ascribed to π-π stacking interactions. Regarding the fluorescence emission spectra, it is noted that for the phosphorescent host compounds synthesized by varying the linking position of the biphenyl groups, corresponding shoulder peaks are observed at longer wavelengths. For instance, the compounds **mCzmBI**, **mCzoBI**, and **oCzmBI** all exhibited a shoulder peak at 362 nm. This observation indicates a certain degree of intramolecular energy transfer within the compounds, driven by electron push-pull interactions. Nevertheless, the maximum emission wavelength of all compounds did not exceed 450 nm.

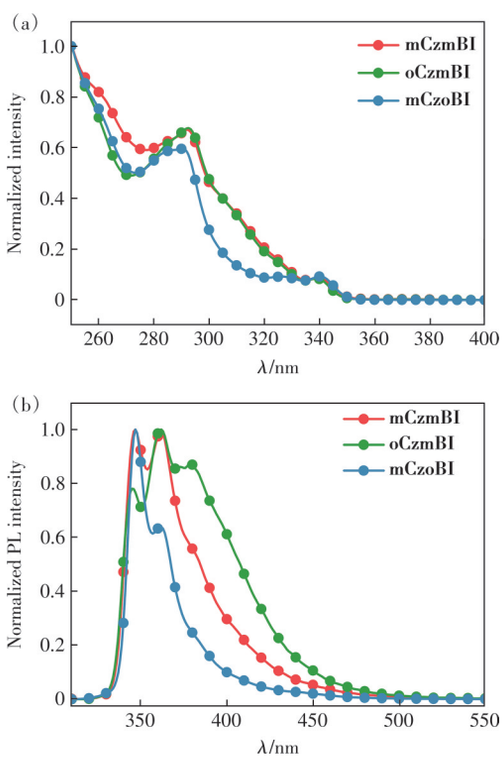

Fig.2 Absorption (upper) and emission spectra (lower) of **mCzmBI**, **mCzoBI** and **oCzmBI** in CH_2Cl_2 solution (5×10^{-6} mol·L^{-1}), respectively

Fig. 3 shows the phosphorescence emission spectra of benzimidazole- and carbazole-based bipolar phosphorescent host compounds in 2-methyltetrahydrofuran solution. The bipolar phosphorescent host compounds with different biphenyl substitution positions exhibit relatively indistinct peak shapes, which is attributed to the small energy level difference between them. The triplet energy levels of all compounds are listed in Tab. 1. It can be observed from Tab. 1 that the triplet energy levels of all compounds are higher than that of the blue phosphorescent guest FIrpic (2.65 eV). Thus, all host compounds are suitable for constructing the blue phosphorescent devices. Consistent with the design goal of this study, the introduction of electron-donating/withdrawing groups and the variation of the biphenyl linking position would increase the electron mobility of the compounds while maintaining their triplet energy levels.

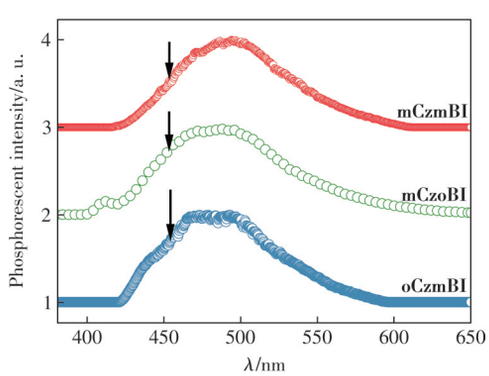

Fig. 3 Phosphorescent spectra of **mCzmBI**, **mCzoBI** and **oCzmBI** in 2-methyltetrahydrofuran at 77 K

Tab. 1　Photophysical data for the compounds mCzmBI, mCzoBI and oCzmBI

Compound	UV/nm[a]	PL/nm[a]	E_g/eV[b]	HOMO/LUMO/eV[c]		HOMO/LUMO/eV[d]		E_T/eV[e]	T_g/T_d/℃[f]
mCzmBI	340/292	362/347	3.5	−5.7	−2.2	−5.5	−2.4	2.70	92/323
mCzoBI	340/292	379/362/345	3.6	−5.7	−2.1	−5.3	−2.1	2.70	103/344
oCzmBI	340/290	362/347	3.6	−5.8	−2.2	−5.3	−2.2	2.70	93/372

[a]Test in dichloromethane solution. [b]Calculated from the onset peak of the UV-Vis absorption spectrum. [c]Measured *via* CV in dichloromethane solution. [d]Calculated using DFT theory. [e]Measured in 2-MeTHF solution at 77 K. [f]Measured *via* DSC and TGA.

2.3　Electrochemical Properties

The highest occupied molecular orbital (HOMO) and lowest unoccupied molecular orbital (LUMO) energy levels of the phosphorescent host compounds were determined *via* CV. A classic three-electrode cell was used to measure the oxidation potential of the host compounds, and the HOMO energy levels were further calculated based on these measured oxidation potentials. Meanwhile, the LUMO energy levels of the compounds were further derived based on the UV-Vis absorption energy gaps and the HOMO values. The measurements were performed under the following conditions: a platinum rod electrode as the counter electrode, an Ag/Ag^+ electrode as the reference electrode, and a platinum-carbon electrode as the working electrode. Tetrabutylammonium perchlorate was used as the electrolyte, and all phosphorescent host compounds (≈ 8 mg/mL) were scanned in deoxygenated (by nitrogen purging) and freshly distilled dry dichloromethane at a scan rate of 50 $mV \cdot s^{-1}$. Since the Ag/Ag^+ electrode was used as the reference electrode, the HOMO energy level (E_{HOMO}) of the compounds was calculated using the formula: $E_{HOMO}=-(4.65+E_{ox})$, where E_{ox} represented the measured oxidation potential of the compound. The scanning results are shown in Fig. 4. Owing to the similar composition of the compounds, their redox peaks of oxidation potential exhibited a similar shape. However, their actual potential values were different (see Tab. 1). It can be observed from Tab. 1 that the HOMO energy levels varied with different linking positions of the biphenyl groups. The HOMO/LUMO energy levels remain essentially unchanged when the linking position of the biphenyl group is altered.

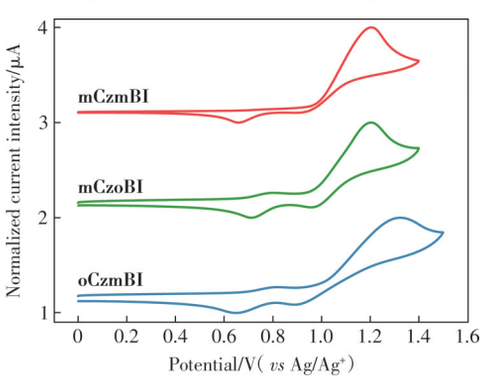

Fig.4　Electrochemical properties of **mCzmBI**, **mCzoBI** and **oCzmBI**

2.4　Thermodynamic Properties

For PhOLEDs fabricated *via* vacuum evaporation, the thermal stability of phosphorescent hosts is closely related to the performance of the devices. Generally, a higher glass transition temperature (T_g) of the host compound leads to relatively better film-forming ability, which in turn contributes to the higher device efficiency. The T_g and thermal decomposition temperatures (T_d) of the biphenyl-linked carbazole-based phosphorescent host compounds were measured using a DSC and a TGA, respectively. Their heat flow curves and mass change curves are presented in Fig. 5, while the specific temperature values are listed in Tab. 1.

As shown in Tab. 1, all benzimidazole- and carbazole-based host compounds exhibit excellent thermal stability, with their T_gs and 5% T_ds exceeding 92 ℃ and 450 ℃, respectively. For the compounds **mCzmBI**, **mCzoBI**, and **oCzmBI**, altering the linking position of the biphenyl groups results in a twisted molecular structure, which can reduce intermolecular stacking and enhance the glass transition temperature. In addition to the rigidity of the linking groups, the thermal stability of the molecules is also strongly related to the asymmetry of the overall molecular structure and changes in polarity.

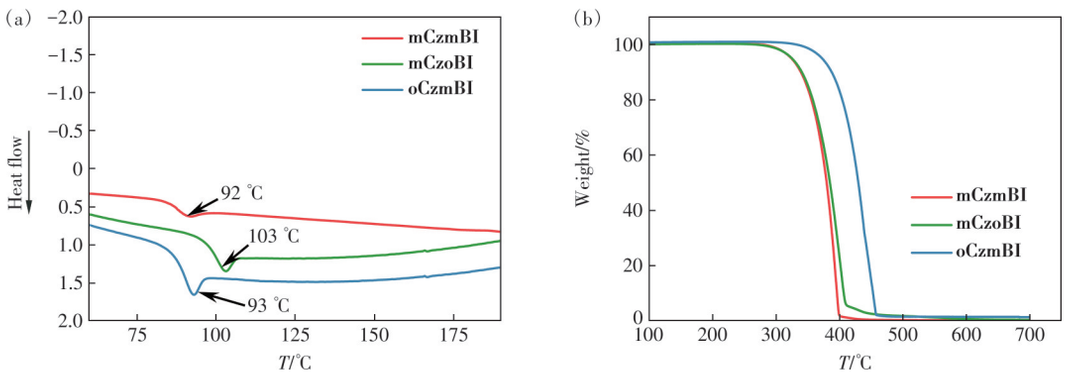

Fig. 5 DSC (left) and TGA (right) curves of the compounds **mCzmBI**, **mCzoBI** and **oCzmBI**

2.5 Theoretical Simulation

The electron cloud distribution of the HOMO and LUMO energy levels in the host compounds allows for an intuitive observation of the key factors influencing the compound energy levels, which holds significant guiding significance for the design of device structures. The molecular structures were optimized using density functional theory (DFT) with ADF2009.01, and the electron cloud distributions of the HOMO/LUMO energy levels as well as the values of the HOMO/LUMO energy levels were calculated. The energy level values are listed in Tab. 1, while Fig. 6 presents the energy level diagrams of the biphenyl-benzimidazole- and carbazole-based bipolar phosphorescent host compounds.

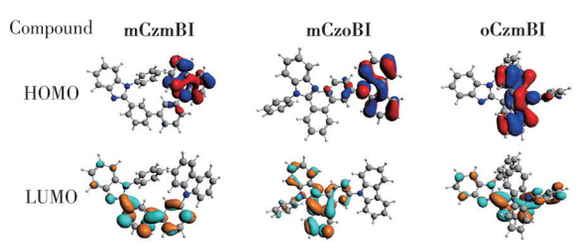

Fig.6 Calculated HOMO and LUMO orbitals of **mCzmBI**, **mCzoBI** and **oCzmBI**

As shown in Fig. 6, the electron cloud of the HOMO energy level of the compounds is mainly distributed on the carbazole moiety, while the electron cloud of the LUMO energy level is primarily localized on the benzimidazole moiety. As the substitution position of the two groups changes from meta to ortho, the degree of overlap between the electron clouds of the HOMO and LUMO energy levels decreases progressively. These results indicate that, with the substituents remaining unchanged, altering the linking position of the biphenyl groups can effectively modulate the HOMO and LUMO energy levels of the compounds, enabling favorable energy level matching with the guest dopant. The calculated HOMO and LUMO energy levels range from −5.3 eV to −5.5 eV and −2.1 eV to −2.4 eV, respectively, and their variation trends are consistent with those of the HOMO and LUMO energy levels obtained *via* CV measurements.

2.6 Electroluminescence Performance

The triplet energy levels of biphenyl-benzimidazole- and carbazole-based bipolar indicate that all host compounds are high enough for blue phosphorescent devices. Therefore, the phosphorescent devices were fabricated *via* vacuum evaporation by using FIrpic as the guest emitter. The devices were constructed as follows: Indium tin oxide (ITO)/Molybdenum trioxide (MoO_3) (10 nm)/N, N′-Bis (1-naphthalenyl)-N, N′-bisphenyl-(1, 1′-biphenyl)-4, 4′-diamine (NPB) (40 nm)/9, 9′-(1, 3-Phenylene) bis-9H-carbazole (mCP) (5 nm)/Host∶6% FIrpic (20 nm)/3, 3′-[5′-[3-(3-Pyridinyl) phenyl][1, 1′∶3′, 1″-terphenyl]-3, 3″-diyl]bispyridine(TmPyPB)(40 nm)/lithium fluoride (LiF)(1 nm)/Al(100 nm)(where the hosts were **mCzmBI** for Device A, **mCzoBI** for Device B, and **oCzmBI** for Device C, respectively). The devices were prepared by using the benzimidazole- and carbazole-based host compounds doped with the blue-light phosphorescent dopant FIrpic to form the phosphorescent emission layer, incorporating a 5 nm-thick mCP layer as the exciton-blocking layer and TmPyPB as the electron-transporting layer. The electroluminescent properties of Devices A−C, are shown in Fig. 7.

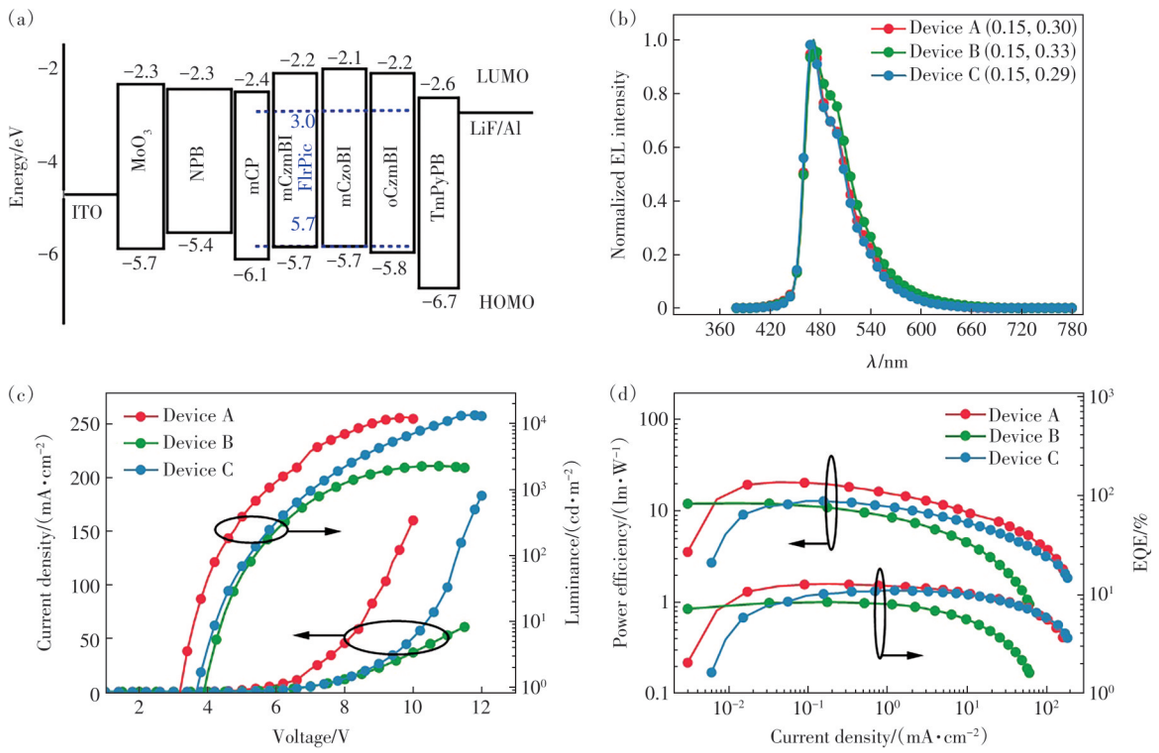

Fig.7　Electroluminescent performances of the devices A–C. (a) Energy level diagrams of each compound in blue phosphorescent devices (Devices A–C). (b) Normalized EL spectra of the devices. (c) *J-V-L* characteristics. (d) External quantum efficiency and power efficiency *versus* current density curves, respectively

Critical device parameters are compiled in Tab. 2. Based on the data shown in Fig. 7 and Tab. 2, the spectral broadening observed in Device B might stem mainly from the exciton recombination zone shifting away from the emissive layer. As indicated in Tab. 1 and Fig. 7(a), **mCzoBI** has poor energy level alignment with the neighboring layers. This misalignment compels excitons to recombine outside the emissive layer or induces interfacial interactions, *e. g.*, exciplex, resulting in non-radiative recombination and emission broadening——consequently increasing the full width at half maximum (FWHM). Furthermore, poor energy level matching with adjacent layers generally raises the injection barriers for electrons and holes, ultimately resulting in a comparatively high device turn-on voltage. In contrast, Device A(with **mCzmBI** as the host) achieves superior energy level alignment, delivering a maximum current efficiency of 24. 9 cd·A^{-1}, power efficiency of 20. 7 lm·W^{-1}, and external quantum efficiency of 12. 8%. Electroluminescence spectra reveal that all three blue phosphorescent devices display intrinsic emission peaks corresponding to FIrpic, with spectral stability maintained across different driving voltages. For devices based on these bipolar phosphorescent hosts, maximum efficiency is attained at relatively high luminance, and efficiency roll-off is mitigated at elevated luminance. These findings demonstrate that biphenyl-linked bipolar blue phosphorescent hosts can effectively suppress device efficiency roll-off under high-luminance operation.

Tab. 2　Device performances of blue phosphorescent organic light-emitting diodes with different bipolar hosts[a]

Device	Host	V_{on}/V[a]	L_{max}/(cd·m^{-2})[b](V/V at L_{max})	H_c[c]/(cd·A^{-1})	H_p[d]/(lm·W^{-1})	EQE[e]/%	FWHM/nm	CIE(x, y)[f]
A	**mCzmBI**	3. 2	12 480 (9. 8)	24. 9	20. 7	12. 8	51	(0. 15,0. 30)
B	**mCzoBI**	3. 8	2 274 (10. 5)	16. 6	12. 1	8. 4	58	(0. 15,0. 33)
C	**oCzmBI**	3. 7	13 410 (11. 6)	20. 2	12. 8	11. 0	50	(0. 15,0. 29)

[a]Operating voltage at a luminance of 1 cd/m^2. [b]Maximum luminance. [c]Maximum current efficiency. [d]Maximum power efficiency. [e]Maximum external quantum efficiency. [f]CIE 1931 color coordinates.

Fig. 7(a) illustrates the HOMO/LUMO energy level diagram of each functional layer in Devices A–C. For all benzimidazole- and carbazole-derived host compounds, minor variations in HOMO/LUMO levels were observed with adjustments to substituent position and type. A key observation is the relatively large energy barrier between the LUMO of all bipolar phosphorescent hosts and the electron-transporting layer (TmPyPB). This barrier restricts electron injection and transport, which in turn contributes to the high turn-on voltages of the devices. Conversely, the HOMO levels of the hosts are well-matched with that of NPB, enabling efficient hole injection from NPB into the emission layer. Additionally, the HOMO/LUMO energy level ranges of all hosts fully cover those of the guest dopant FIrpic; this favorable alignment facilitates energy transfer from host to guest, thereby improving the efficiency of phosphorescent OLEDs.

The efficiency data of all the above devices indicate that benzimidazole- and carbazole-based bipolar phosphorescent host compounds are suitable for the FIrpic-based devices. By introducing different numbers of electron-type groups and adjusting the linking positions of benzimidazole and carbazole on the biphenyl group, we can effectively modulate the electroluminescent performance of the device with such host compounds.

3 Conclusion

In summary, a series of bipolar blue phosphorescent host materials based on benzimidazole and carbazole were designed and synthesized. By precisely tuning the electron-withdrawing groups and the linking positions of biphenyl moieties, the spectral, electrochemical, and thermodynamic properties, as well as the bipolar transport performance, of these host materials were optimized. The blue phosphorescent guest FIrpic exhibited good compatibility with all three bipolar hosts. Notably, compared with devices using **mCzoBI** and **oCzmBI** (with ortho-linkage) as hosts, the device based on **mCzmBI**——where carbazole and benzimidazole groups are linked to the biphenyl moiety *via* double meta positions——showed a lower turn-on voltage, higher device efficiency, and better efficiency roll-off performance. Owing to its excellent carrier transport properties, the **mCzmBI**-based device achieved a maximum external quantum efficiency of 12.8%. These findings provide a valuable guideline for the development of high-performance phosphorescent host materials.

Supplementary Information and Response Letter are available for this paper at: http://cjl.lightpublishing.cn/thesisDetails#10.37188/CJL.20250223

Reference:

[1] BALDO M A, O'BRIEN D F, YOU Y, *et al*. Highly efficient phosphorescent emission from organic electroluminescent devices [J]. *Nature*, 1998, 395(6698): 151-154.

[2] PORIEL C, RAULT-BERTHELOT J. Designing host materials for the emissive layer of single-layer phosphorescent organic light-emitting diodes: toward simplified organic devices [J]. *Adv. Funct. Mater.*, 2021, 31(24): 2010547.

[3] WANG Y X, YUN J H, WANG L, *et al*. High triplet energy hosts for blue organic light-emitting diodes [J]. *Adv. Funct. Mater.*, 2021, 31(12): 2008332.

[4] LI D L, LI J Y, LIU D, *et al*. Highly efficient simple-structure sky-blue organic light-emitting diode using a bicarbazole/cyanopyridine bipolar host [J]. *ACS Appl. Mater. Interfaces*, 2021, 13(11): 13459-13469.

[5] CHENG C Q, ZHU S Q, ZHANG H, *et al*. Tailoring indolocarbazole-bridged multiple resonance emitter through steric presubstitution for narrowband electroluminescence with EQE over 40% [J]. *Angew. Chem. Int. Ed.*, 2025, 64(39): e202504628.

[6] SONG W X, XU Q H, ZHU J N, *et al*. Imidazo[1,2-*b*]pyridazine as building blocks for host materials for high-performance red-phosphorescent organic light-emitting devices [J]. *ACS Appl. Mater. Interfaces*, 2020, 12(17): 19701-19709.

[7] TANG X, LIU X Y, YUAN Y, *et al*. High-efficiency white organic light-emitting diodes integrating gradient exciplex allocation system and novel D-Spiro-A materials [J]. *ACS Appl. Mater. Interfaces*, 2018, 10(35): 29840-29847.

[8] LUCAS F, QUINTON C, FALL S, *et al*. Universal host materials for red, green and blue high-efficiency single-layer phosphorescent organic light-emitting diodes [J]. *J. Mater. Chem.* C, 2020, 8(46): 16354-16367.

[9] KANG J, MOON J, JEON S O, *et al*. Diindolocarbazole as a core structure for narrow-emitting and highly efficient blue organic light-emitting diodes [J]. *Adv. Sci.*, 2025, 12(32): e04625.
[10] UDAGAWA K, SASABE H, CAI C, *et al*. Low-driving-voltage blue phosphorescent organic light-emitting devices with external quantum efficiency of 30% [J]. *Adv. Mater.*, 2014, 26(29): 5062-5066.
[11] LUCAS F, IBRAIKULOV O A, QUINTON C, *et al*. Spirophenylacridine-2,7-(diphenylphosphineoxide)-fluorene: a bipolar host for high-efficiency single-layer blue phosphorescent organic light-emitting diodes [J]. *Adv. Opt. Mater.*, 2020, 8(2): 1901225.
[12] MONKMAN A. Why do we still need a stable long lifetime deep blue OLED emitter? [J] *ACS Appl. Mater. Interfaces*, 2022, 14(18): 20463-20467.
[13] CHAN C Y, TANAKA M, LEE Y T, *et al*. Stable pure-blue hyperfluorescence organic light-emitting diodes with high-efficiency and narrow emission [J]. *Nat. Photonics*, 2021, 15(3): 203-207.
[14] KIM M, RYU C H, PARK H Y, *et al*. Nido-ortho-carborane-functionalized salt-type tetradentate Pt(II) complexes and their application as blue phosphors in efficient organic light-emitting diodes [J]. *Adv. Opt. Mater.*, 2025, 13(26): e01083.
[15] ABROSHAN H, COROPCEANU V, BRÉDAS J L. Hyperfluorescence-based emission in purely organic materials: suppression of energy-loss mechanisms *via* alignment of triplet excited states [J]. *ACS Materials Lett.*, 2020, 2(11): 1412-1418.
[16] SONG X J, LI X N, YE X Y, *et al*. Alleviated efficiency roll-off in organic light-emitting diode through optimizing peripheral substituents in multiple-resonance thermally activated delayed fluorescence material [J]. *Adv. Opt. Mater.*, 2025, 13(19): 2500515.
[17] PORIEL C, RAULT-BERTHELOT J, JIANG Z Q. Are pure hydrocarbons the future of host materials for blue phosphorescent organic light-emitting diodes? [J]. *Mater. Chem. Front.*, 2022, 6(10): 1246-1252.
[18] ELGADI S A, MIKULIN S, HUDSON Z M. Recent progress in organic TADF emitters containing heavy atoms [J]. *Adv. Opt. Mater.*, 2025, 13(21): 2500683.
[19] WANG J J, LI N Q, ZHONG C, *et al*. Metal-perturbed multiresonance TADF emitter enables high-efficiency and ultralow efficiency roll-off nonsensitized OLEDs with pure green gamut [J]. *Adv. Mater.*, 2023, 35(6): 2208378.
[20] PORIEL C, RAULT-BERTHELOT J. Blue single-layer organic light-emitting diodes using fluorescent materials: a molecular design view point [J]. *Adv. Funct. Mater.*, 2020, 30(17): 1910040.
[21] MERTENS R. *The OLED Handbook* [M/OL]. 2025-10-13. https://www.oled-info.com/oled-handbook-2021-edition.
[22] LI Y C, LIU J Y, ZHAO Y D, *et al*. Recent advancements of high efficient donor-acceptor type blue small molecule applied for OLEDs [J]. *Mater. Today*, 2017, 20(5): 258-266.
[23] PAN B, WANG B, WANG Y X, *et al*. A simple carbazole-*N*-benzimidazole bipolar host material for highly efficient blue and single layer white phosphorescent organic light-emitting diodes [J]. *J. Mater. Chem. C*, 2014, 2(14): 2466-2469.
[24] LAI M Y, CHEN C H, HUANG W S, *et al*. Benzimidazole/amine-based compounds capable of ambipolar transport for application in single-layer blue-emitting OLEDs and as hosts for phosphorescent emitters [J]. *Angew. Chem. Int. Ed.*, 2008, 47(3): 581-585.
[25] SONG W, LEE J Y. Degradation mechanism and lifetime improvement strategy for blue phosphorescent organic light-emitting diodes [J]. *Adv. Opt. Mater.*, 2017, 5(9): 1600901.
[26] PENCONI M, CAZZANIGA M, PANZERI W, *et al*. Unraveling the degradation mechanism in FIrpic-based blue OLEDs: Ⅱ. trap and detect molecules at the interfaces [J]. *Chem. Mater.*, 2019, 31(7): 2277-2285.
[27] SCHMIDBAUER S, HOHENLEUTNER A, KÖNIG B. Chemical degradation in organic light-emitting devices: mechanisms and implications for the design of new materials [J]. *Adv. Mater.*, 2013, 25(15): 2114-2129.
[28] SON H S, LEE J Y. Structure-property relationship in high triplet energy host materials with a phenylcarbazole core and diphenylphosphine oxide substituent [J]. *Org. Electron.*, 2011, 12(6): 1025-1032.

黄宏(1985-),男,湖南邵阳人,博士,高级工程师,2012年于华中科技大学获得博士学位,主要从事有机电致发光材料与器件的研究。
E-mail: huangxiaoli1985@126.com

谢国华(1982-),男,福建漳州人,博士,教授,博士生导师,2011年于吉林大学获得博士学位,主要从事有机光电材料与器件的研究。
E-mail: ifeghxie@xmu.edu.cn